Supporting Information

Building Carbon Cloth-Based Dendrite-Free Potassium Metal Anodes for Potassium Metal Pouch Cells

Fan Qiao, Jiashen Meng, Junjun Wang, Peijie Wu, Dawei Xu, Qinyou An, Xuanpeng Wang*, Liqiang Mai*

Experimental section

Preparation of K-CC@SnO_2 composite anode. $SnCl_2$ (0.30 g), poly(vinylpyrrolidone) (PVP, K30, 0.10 g) and 1,4-dicarboxybenzene (0.12 g) were successively dissolved in 70 mL of N, N-dimethylformamide (DMF) solvent under stirring at room temperature for 1 h to obtain a colorless transparent solution. The commercial carbon cloth was then fully immersed in the solution and transferred to a 100 mL Teflon-lined stainless-steel autoclave and heated to 180 °C for 12 h. After it cooled down to room temperature, the carbon cloth was collected, washed with methanol three times and dried at 60 °C vacuum drying oven. Subsequently, after complete pyrolysis at 450 °C for 3 h with heating rate of 5 °C min^{-1} in Muffle, the CC@SnO_2 was obtained. The CC@SnO_2 slices were obtained by cutting CC@SnO_2 into disc with a diameter of 10 mm. Finally, facile molten infusion was performed under ~80 °C (Video S1) in an argon-filled glovebox (H_2O, O_2 < 0.1 ppm) to embed K into the CC@SnO_2 slice framework. The K-CC@SnO_2 composite anode was obtained with an average load of 21.40-36.18 mg cm^{-2}. In the pouch cell, the area of the cathode is 23 cm^2 (5.75 cm *4 cm), the active material is 25 mg, the area of the anode is 27 cm^2 (6 cm *4.5 cm) and the amount of electrolyte is 2.5 mL.

Material characterization. XRD patterns were received by a Bruker D8 Discover X-ray diffractometer with Cu Kα radiation source. The SEM images were acquired by a JEOL-7100F microscope. XPS analysis was performed using a VG MultiLab 2000. Fourier transform infrared (FTIR) transmittance spectra were recorded using a Nicolet 6700 (Thermo Fisher Scientific Co., USA) IR spectrometer.

Electrochemical characterization. In the symmetry cells and full cells electrochemical measurements, CR2016-type coin cells were assembled in an argon-filled glove box (H_2O, O_2 < 0.1 ppm), GF/D was used as separator, and 1 M solution of KFSI in ethylene carbonate (EC) and dimethyl carbonate (DEC) (1:1, volume ratio) as the electrolyte. The commercial PTCDI was bought from Alfa Aesar Co. The PTCDI electrodes with an ordinary mass loading (~1.0 mg cm^{-2}) were obtained by casting process. 60 wt% active materials, 30 wt% acetylene black and 10 wt% polyvinylidene fluoride binder were mixed to produce a homogenous slurry. Then the slurry was casted on Al foil with carbon-coated and dried at 70 °C overnight. The electrode slices were obtained by cutting the dried foil into disc with a diameter of 10 mm. Galvanostatic charge/discharge tests were conducted using a LAND CT2001A. Cyclic voltammetry (1.5-3.5 V) and electrochemical impedance spectra were tested using an electrochemical workstation (Autolab PGSTAT302N).

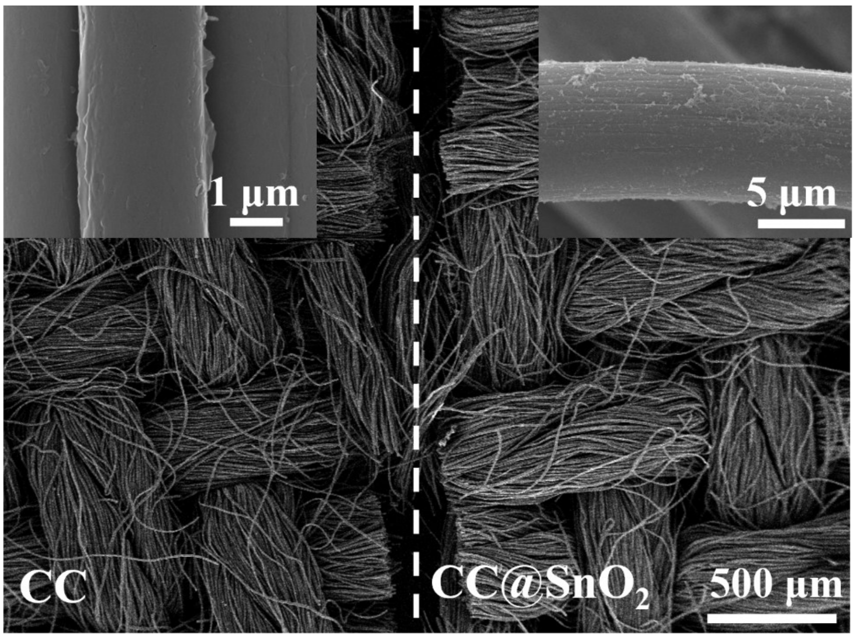

Figure S1. SEM images of CC and $CC@SnO_2$.

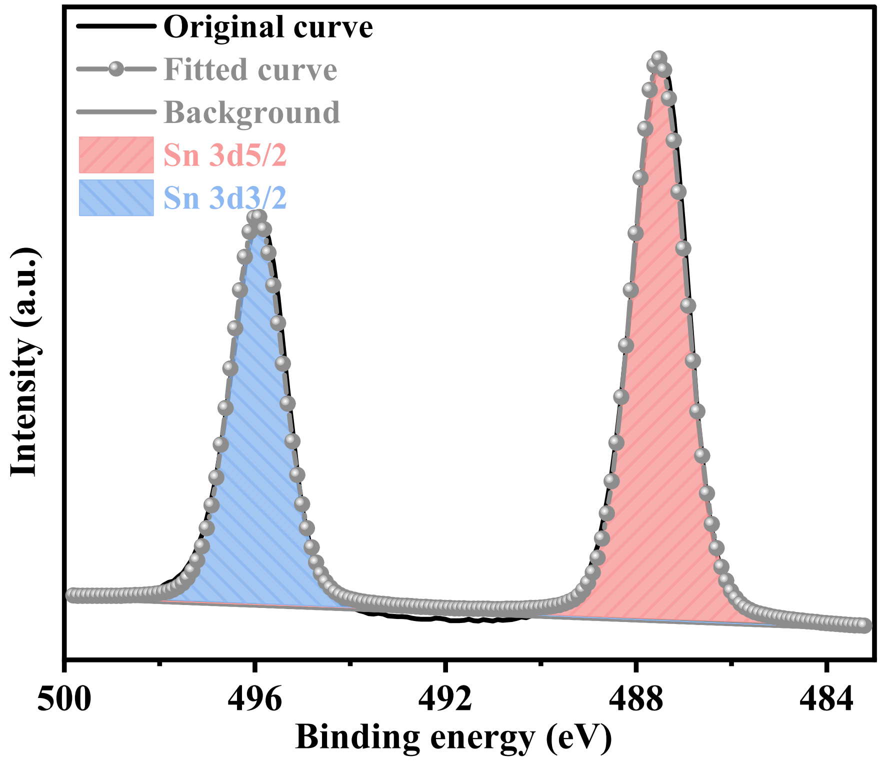

Figure S2. High resolution Sn 3d XPS spectra of CC@SnO_2.

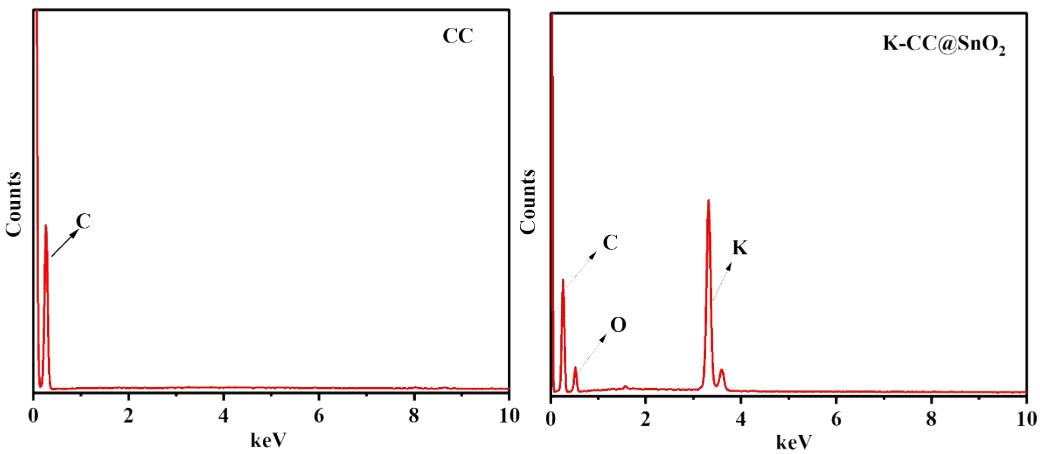

Figure S3. The EDS images of (a) CC and (b) K-CC@SnO_2.

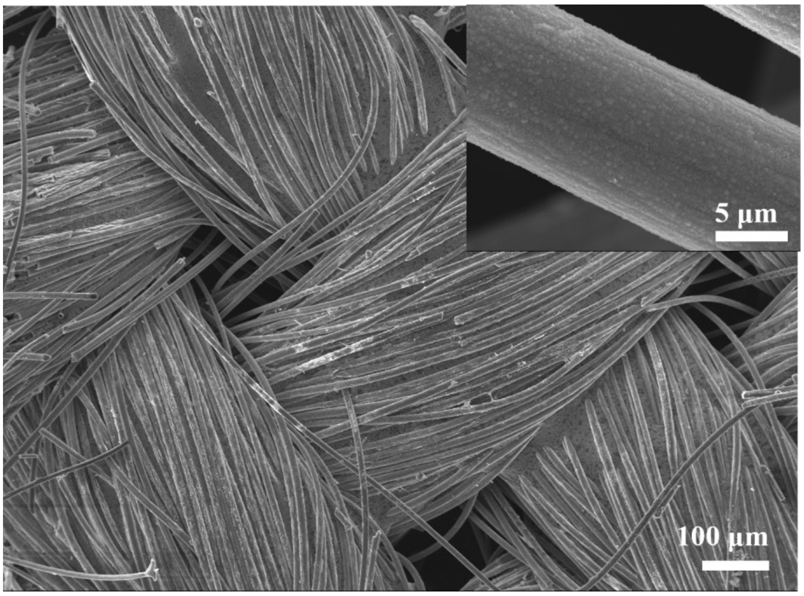

Figure S4. SEM images of K-CC@SnO_2.

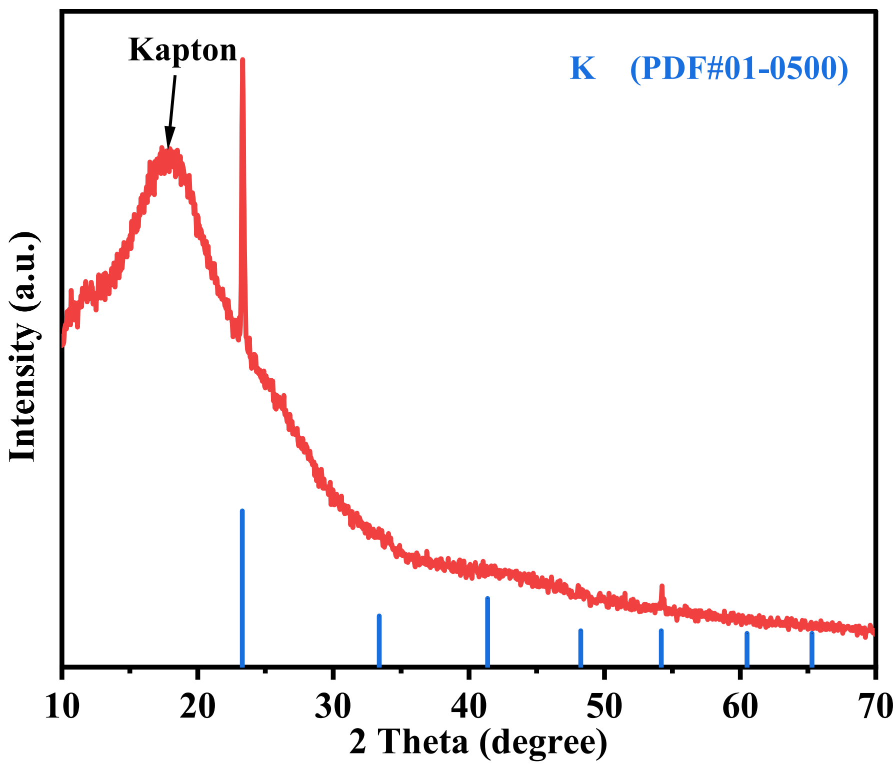

Figure S5. XRD pattern of K-CC@SnO_2.

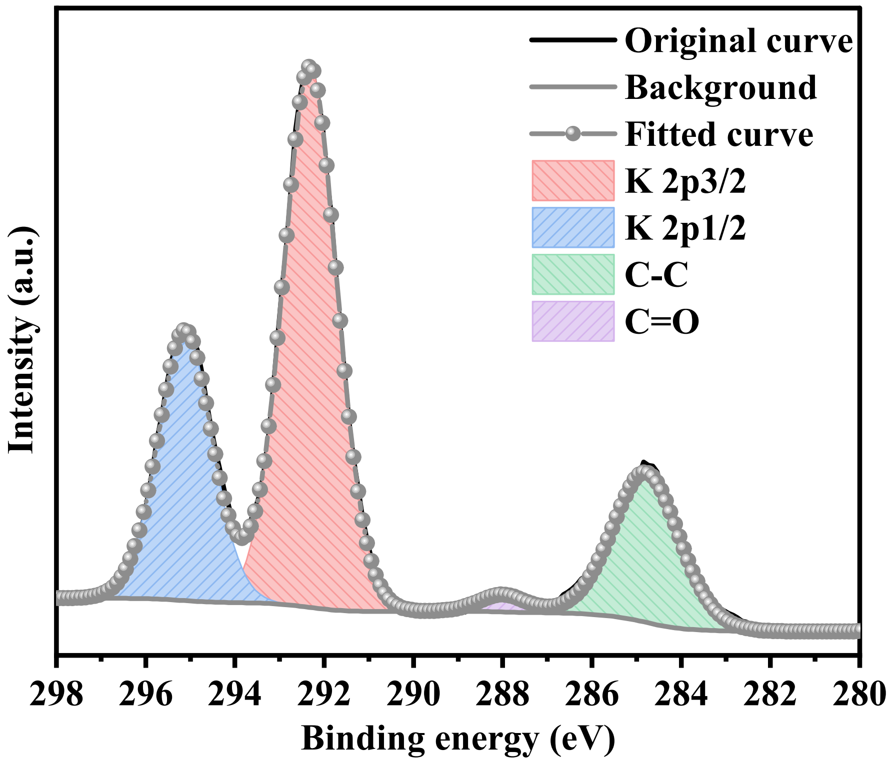

Figure S6. High resolution K 2p and C 1s XPS spectra of K-CC@SnO_2.

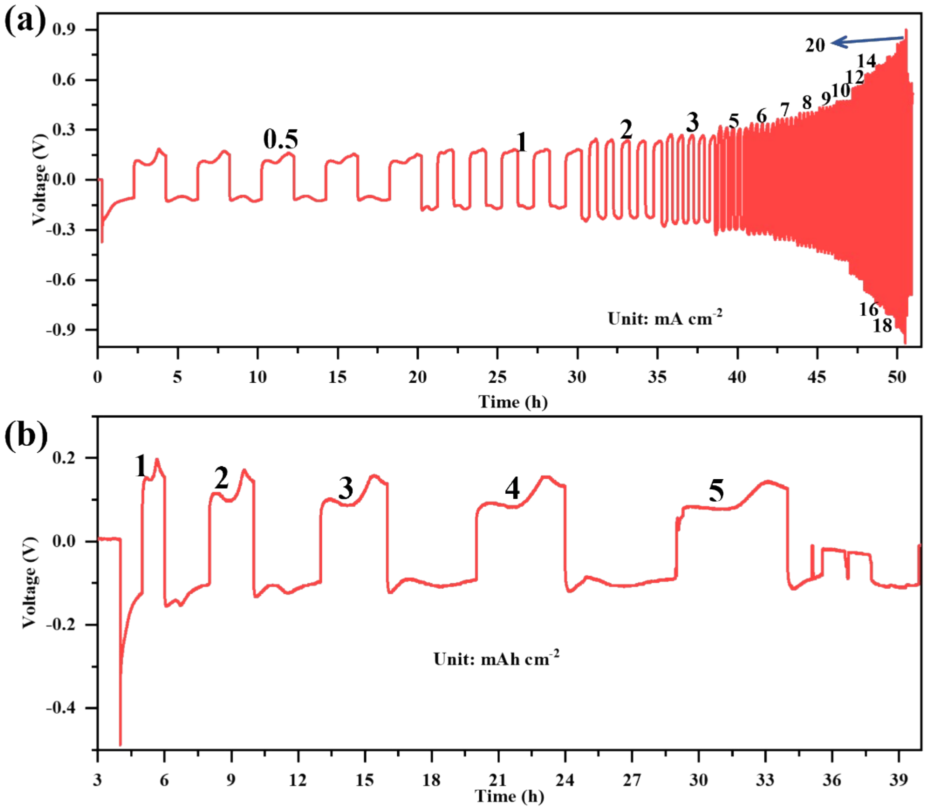

Figure S7. The voltage profile of K-CC@SnO_2 (a) with the capaciy of 1 mAh cm^{-2} at different current densities and (b) with different capaciy at 1 mA cm^{-2}.

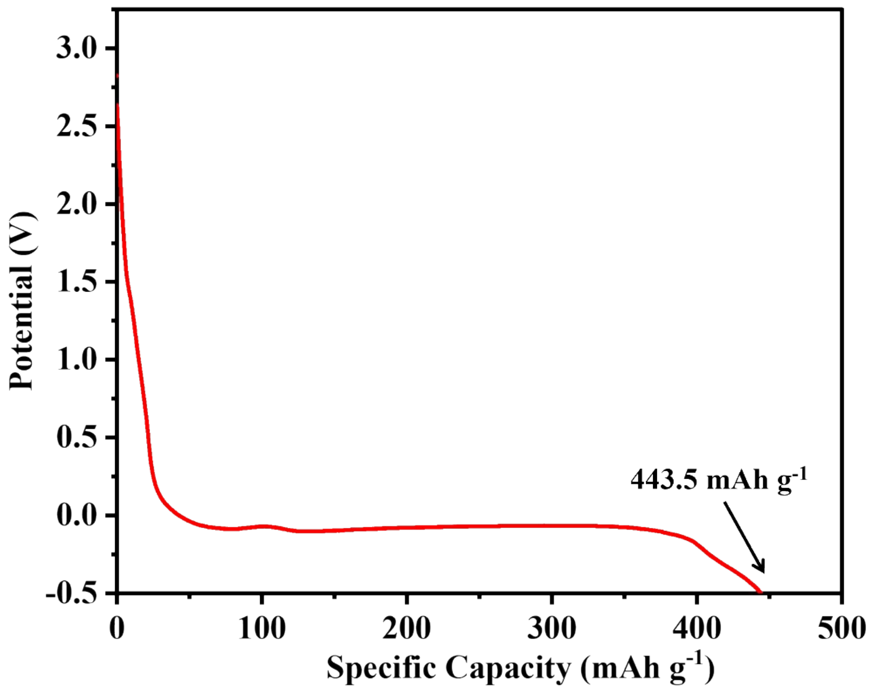

Figure S8. The Discharge curve of K-CC@SnO_2||CC@SnO_2 cell at 1 mA cm^{-2}.

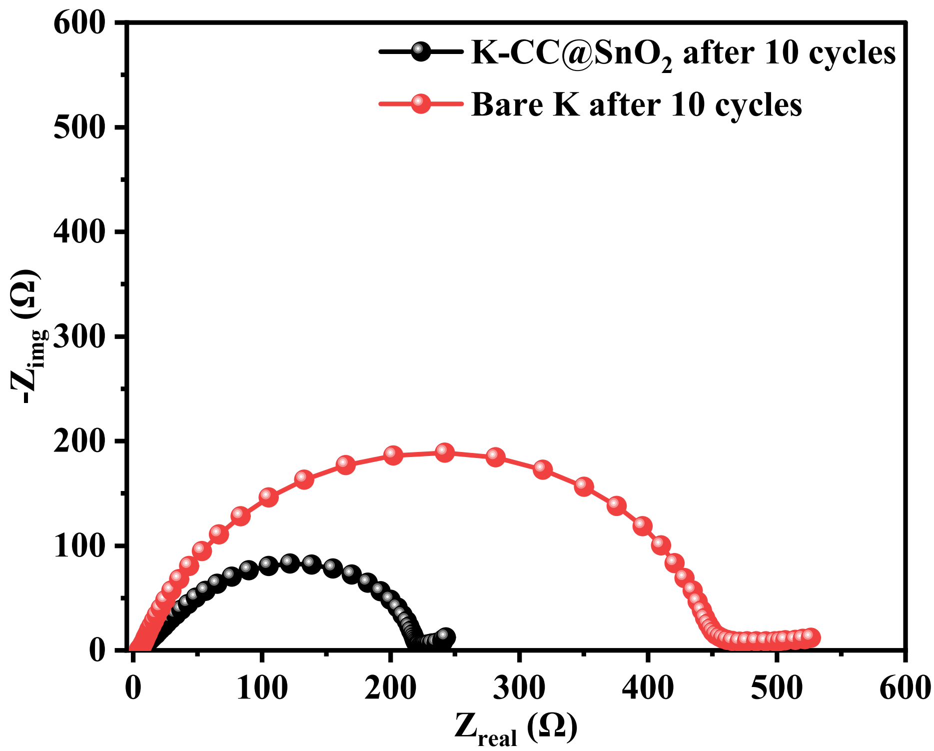

Figure S9. Impedance plots of K||K and K-CC@SnO_2||K-CC@SnO_2 symmetric cells after 10 cycles.

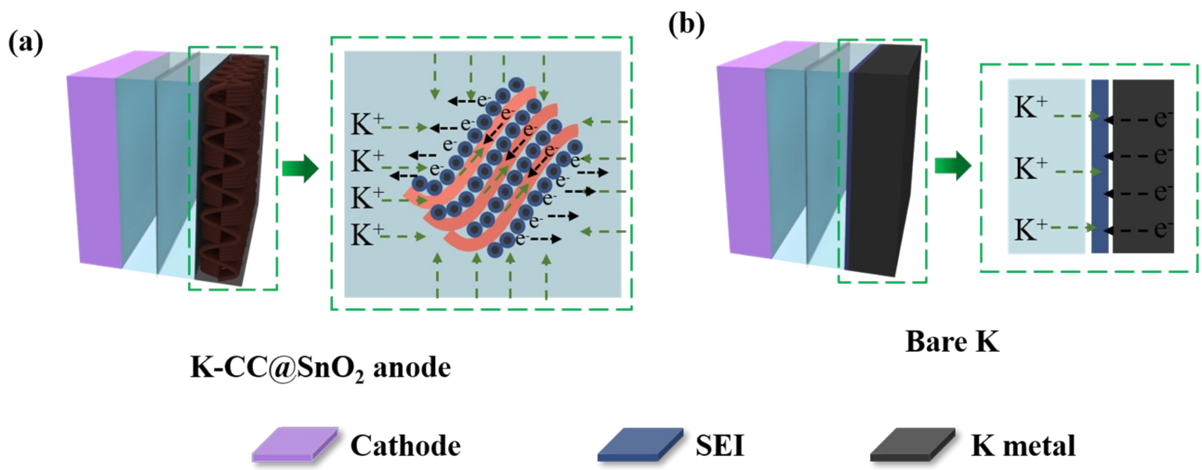

Figure S10. Schematics of ions and electronics network in a K-CC@SnO$_2$ electrode (a) and in a traditional chunk of K metal (b).

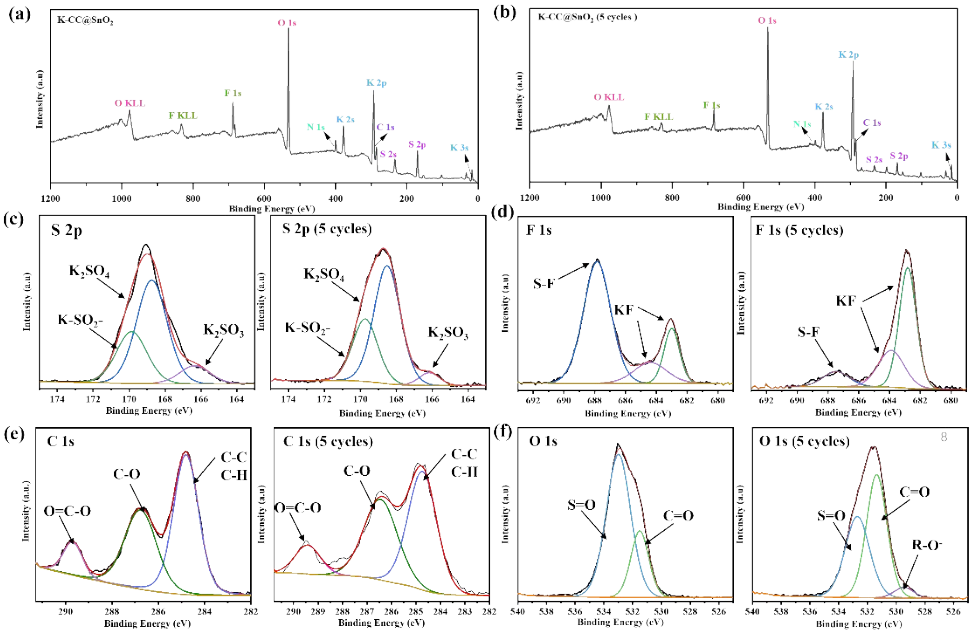

Figure S11. XPS survey spectrum of (a) the initial and (b) cycled K-CC@SnO$_2$ electrode. High-resolution (c) S 2p, (d) F 1s, (e) C 1s and (f) O 1s XPS spectra of the pristine and cycled K-CC@SnO$_2$ electrode.

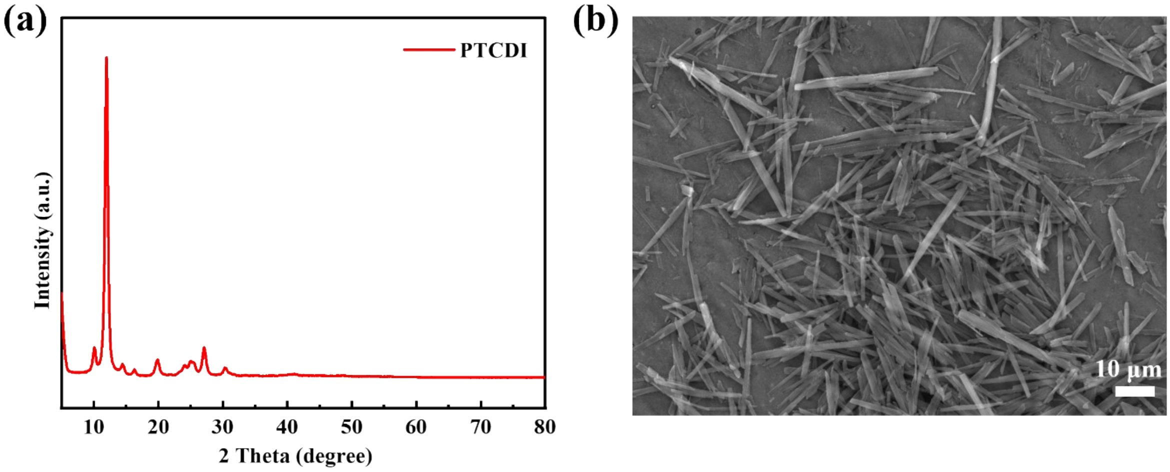

Figure S12. XRD pattern (a) and SEM image (b) of PTCDI.

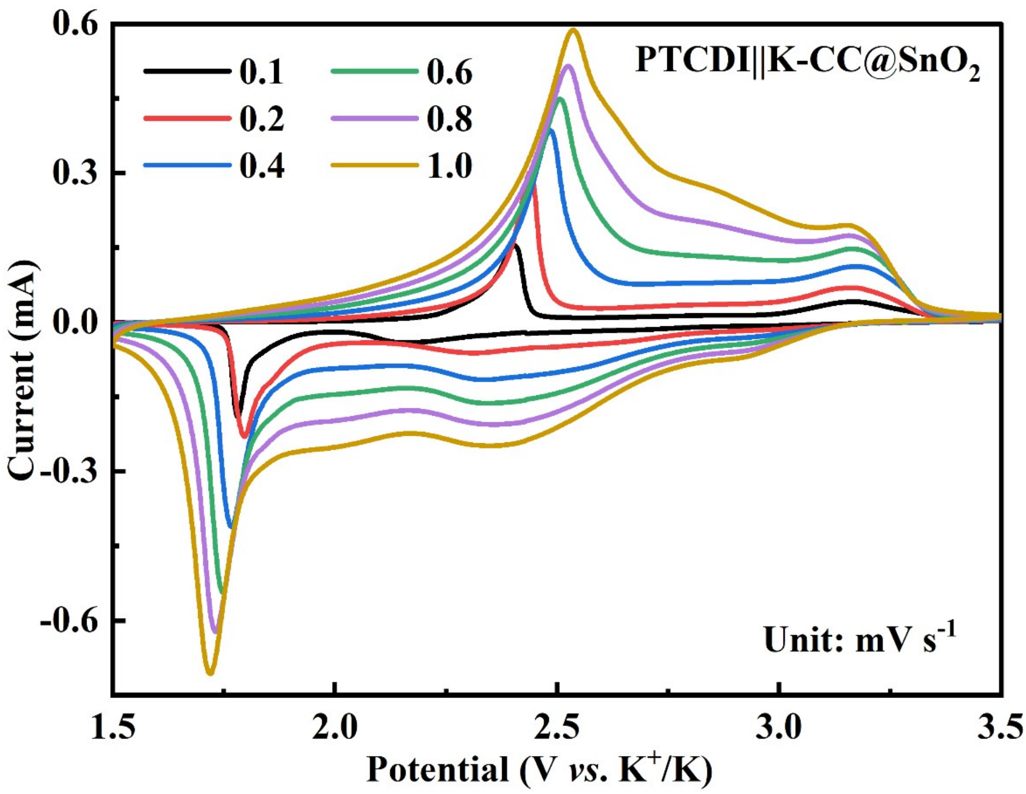

Figure S13. Typical CV curves of the PTCDI||K-CC@SnO_2 cell at various scan rates.

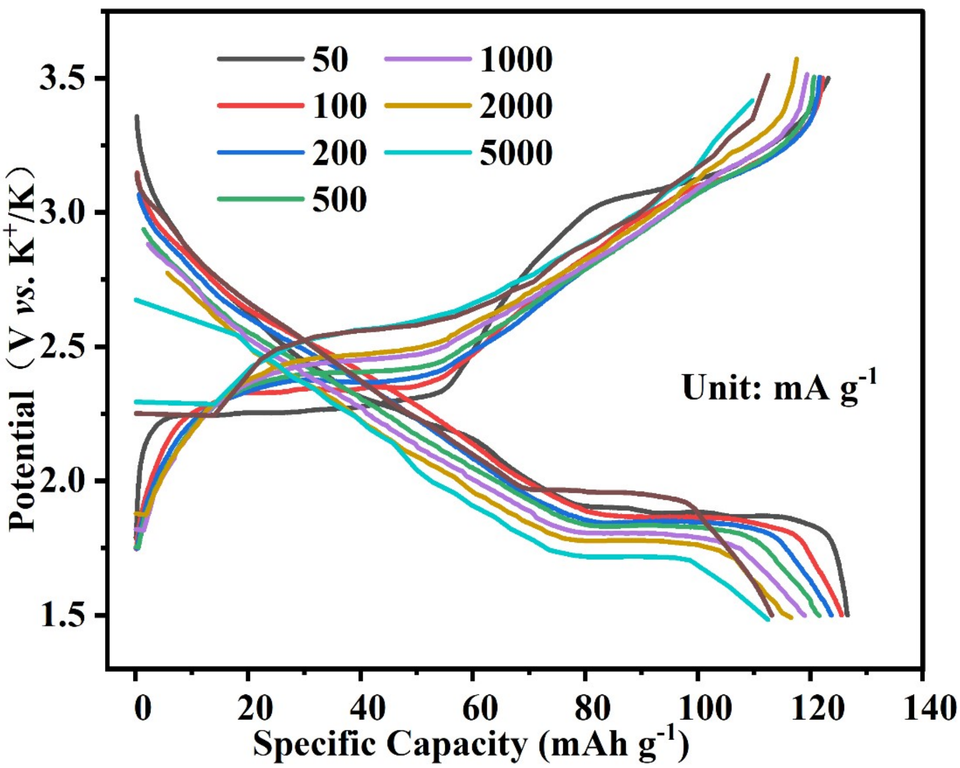

Figure S14. The charge-discharge curves of PTCDI||K- CC@SnO_2 full cell at various current densities.

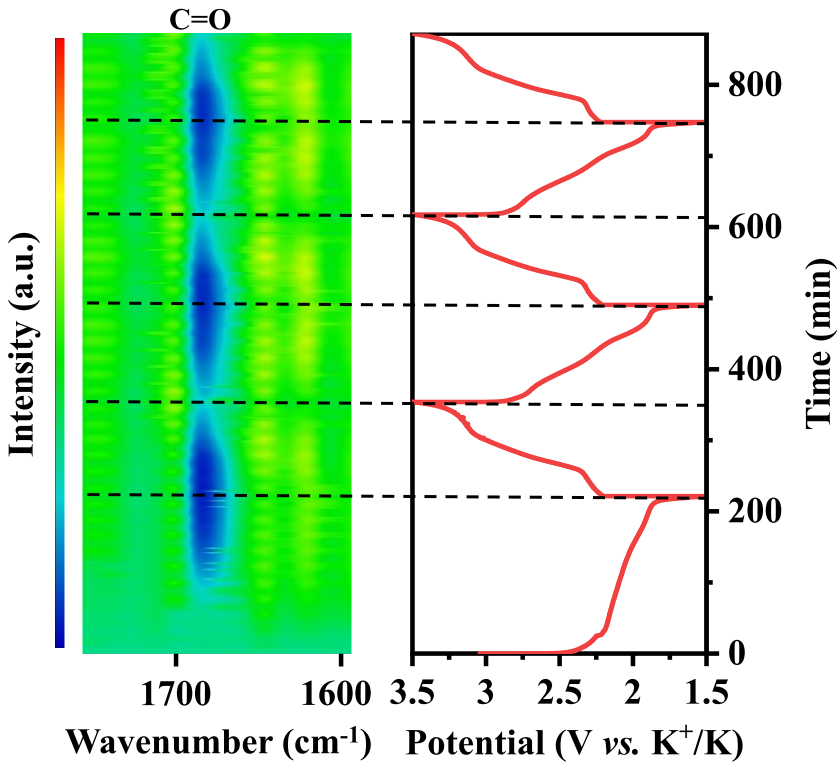

Figure S15. The in-situ FT-IR spectroscopy of PTCDI in the PTCDI||K-CC@SnO_2 full cell.

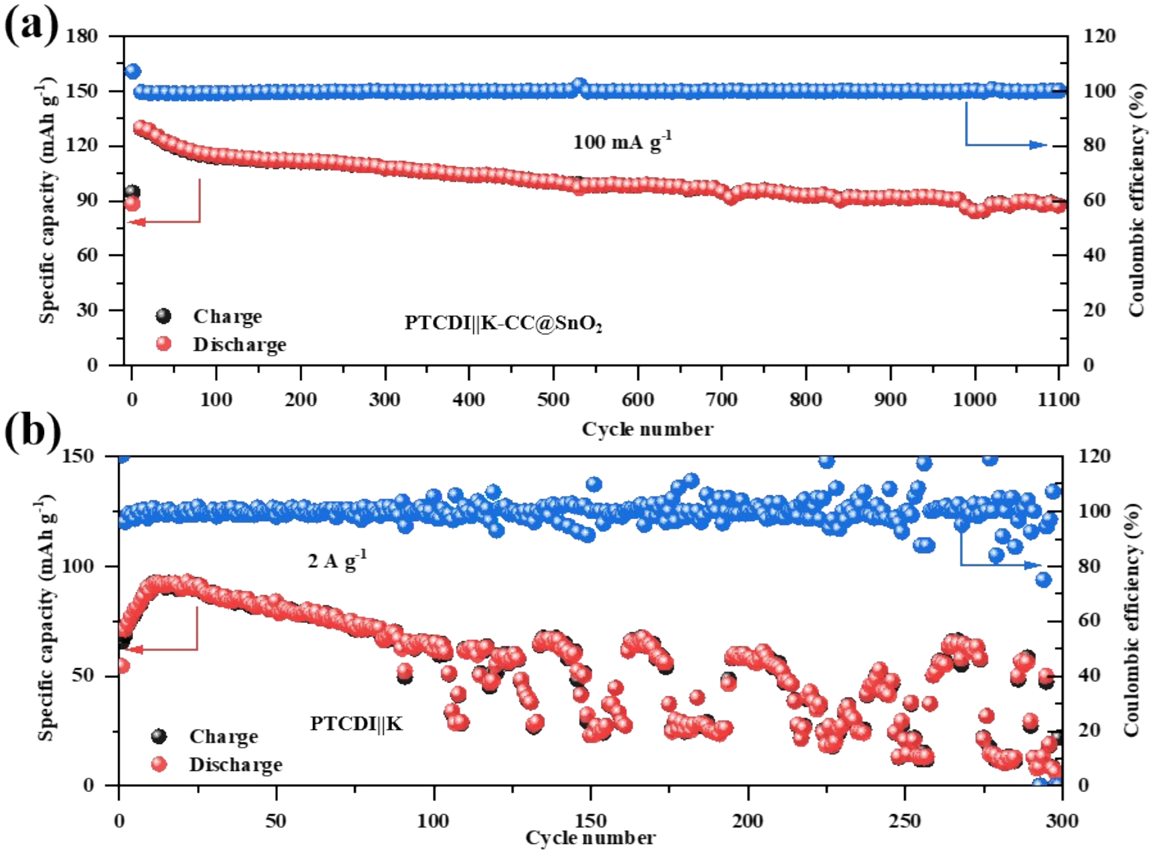

Figure S16. The cycling performance of PTCDI||K-CC@SnO_2 full cell at 100 mA g^{-1} (a) and the cycling performance of PTCDI||K full cell at 2000 mA g^{-1} (b).

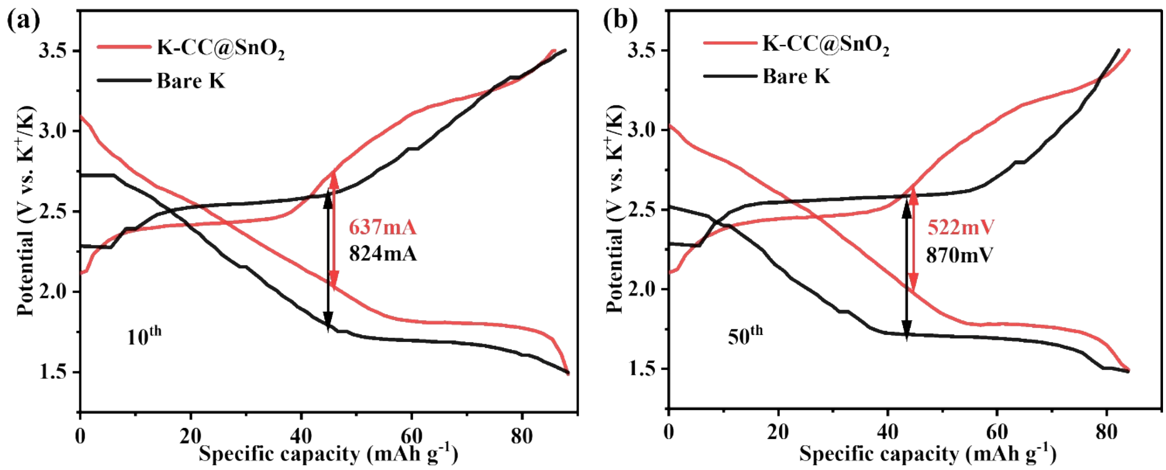

Figure S17. Typical galvanostatic voltage profiles in the 10th (a) and 50th (b) cycles at the current density of 2 A g^{-1}.

Table S1. The summary of OPIBs electrode materials.

Organic electrode materials	Potential window (V)	Electrolyte	Capacity retention (cycle number, current density)	Reference
PTCDI	1.5-3.5	1 M KFSI-EC/DEC	70.9% (10000, 2000 mA g^{-1})	This work
PTCDI	1.4–3.8	5 M KFSI-EC/DMC	87.5% (600, 4000 mA g^{-1})	[1]
PTCDI-DAQ	1.0–3.8	1 M KPF_6-DME/0.05M LiTFSI	76.7% (900, 3 A g^{-1})	[2]
AQDS	1.4–3.0	0.8 M KPF_6-EC/DEC	82.1% (100, 0.1 C)	[3]
o-$Na_2C_6H_2O_6$	1.0–3.0	0.8 M KPF_6-EC/DEC	38.7% (100, 25 mA g^{-1})	[4]
p-$Na_2C_6H_2O_6$	1.0–3.0	0.8 M KPF_6-EC/DEC	47.3% (50, 0.1 C)	[5]
VK@CNT	0.2–2.5	0.8 M KPF_6-EC/DEC	65.6% (100, 100 mA g^{-1})	[6]
PTCDA	1.5–3.5	0.5 M KPF_6-EC/DEC	77% (200, 10 mA g^{-1})	[7]
K_4PTC@CNTs	0.1–2.0	1 M KFSI-EC/DMC	73.5% (500, 50 mA g^{-1})	[8]
K_2SBDC	0.1–2.5	1 M KFSI-EC/DMC	124 mAhg@1 (100, 50 mA g^{-1})	[9]
K_2BPDC@GR	0.1–2.5	1 M KFSI-EC/DMC	170 mAh g^{-1} (100, 50 mA g^{-1})	[9]
K_2TP	0.1–2.0	1 M KPF_6-DME	92.0% (100, 200 mA g^{-1})	[10]
K_2PC	0.1–2.0	1 M KFSI-EC/DMC	93% (100, 0.2 C)	[11]
AIBN	0.01–3.0	-	40% (100, 10 mA g^{-1})	[12]
ADAPTS	0.5–3.0 0.5–3.0	0.8 M KPF_6-EC/DEC	79% (400, 1 C) 81% (80, 2 C)	[13]
OHTAP	1.1–3.1	1 M KTFSI-DOL/DME	73.6% (50, 0.1 C)	[14]
PQ-1,5	1.2–3.2	1 M KTFSI-DOL/DME	91% (200, 250 mA g^{-1})	[15]
PQ-1,4	1.2–3.2	1 M KTFSI-DOL/DME	50 mA g^{-1}	[15]
PQ-CN	1.2–3.2	1 M KTFSI-DOL/DME	52.2% (200, 250 mA g^{-1})	[15]
PI@G	1.5–3.5	KFSI-DME (1:5, molar ratio)	83% (500, 100 mA g^{-1})	[16]
PAQS	1.3–3.4	0.5 M KTFSI-DOL/DME	77.2% (200, 200 mA g^{-1})	[17]
PPTS	0.8–3.2	1 M KPF_6-DME	73.7% (3000, 5 A g^{-1})	[18]

PTCDA-kC (k=0, 2, 3, 4)	1.2–3.2 1.2–3.2	5 M KTFSI-DME	75% (1000, 2.21 C, k=0), 94% (1000, 7.35 C, k=2)	[19]
p-DPPZ	2.5–4.5	2.2 M KPF_6-DG	59% (2000, 2 A g^{-1})	[20]
PDPPD	2.5–4.5	0.5 M KPF_6-EC/DEC	86% (500, 1 C)	[21]
PHAT	0.9–3.4	1 M KPF_6-DME	169 mAh g^{-1} (4600, 10 A g^{-1})	[22]
MIL-125(Ti)	0.01–3.0	1 M KFSI-EC/DEC	90.2% (2000, 200 mA g^{-1})	[23]
L-$Co_2(OH)_2$BDC	0.2–3.0	1 M KPF_6-DME	188 mAh g^{-1} (600, 1 Ag^{-1})	[24]
K-MOF $[C_7H_3KNO_4]_n$@CNT	0.1–2.0	1 M KFSI-EC/DMC	92% (300, 100 mA g^{-1})	[25]
MOF-235/MCNTs	0.01–3.0	1 M KFSI-EC/DEC	132 mAh g^{-1} (200, 200 mA g^{-1})	[26]
UCF@CNs@BiN	0.01–3.0	3 M KFSI-DME	77% (600, 100 mA g^{-1})	[27]
CTF-0	0.01–3.0	0.8 M KPF_6-EC/DEC	73.4% (200, 100 mA g^{-1})	[28]
CTF-1	0.01–3.0	0.8 M KPF_6-EC/DEC	60 mAh g^{-1} (200, 100 mA g^{-1})	[28]
COF-10@CNT	0.005–3.0	1 M KFSI-EC/DEC	161 mAh g^{-1} (4000, 1 A g^{-1})	[29]
CMPs	0.1–3.0	0.8 M KPF_6-EC/DEC	272 mAh g^{-1} (500, 50 mA g^{-1})	[30]

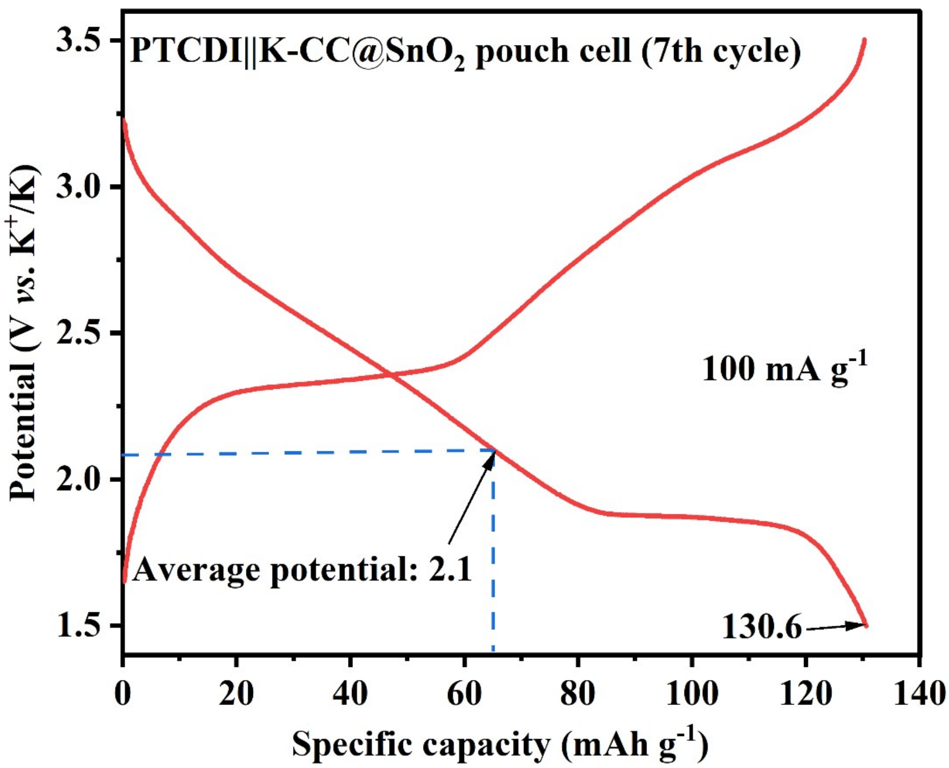

Figure S18. The charge/discharge profiles of PTCDI||K-CC@SnO_2 pouch cell.

[1] M. Xiong, W. Tang, B. Cao, C. Yang and C. Fan, *J. Mater. Chem. A* **2019,** *7*, 20127.
[2] Y. Hu, W. Tang, Q. Yu, X. Wang, W. Liu, J. Hu and C. Fan, *Adv. Funct. Mater.* **2020,** *30*, 2000675.
[3] J. Zhao, J. Yang, P. Sun and Y. Xu, *Electrochem. Commun.* **2018,** *86*, 34.
[4] L. Chen, S. Liu, Y. Wang, W. Liu, Y. Dong, Q. Kuang and Y. Zhao, *Electrochim. Acta* **2019,** *294*, 46.
[5] L. Chen and Y. Zhao, *Mater. Lett.* **2019,** *243*, 69.
[6] Q. Xue, D. Li, Y. Huang, X. Zhang, Y. Ye, E. Fan, L. Li, F. Wu and R. Chen, *J. Mater. Chem. A* **2018,** *6*, 12559.
[7] Y. Chen, W. Luo, M. Carter, L. Zhou, J. Dai, K. Fu, S. Lacey, T. Li, J. Wan, X. Han, Y. Bao and L. Hu, *Nano Energy* **2015,** *18*, 205.
[8] C. Wang, W. Tang, Z. Yao, B. Cao and C. Fan, *Chem. Commun.* **2019,** *55*, 1801.
[9] C. Li, Q. Deng, H. Tan, C. Wang, C. Fan, J. Pei, B. Cao, Z. Wang and J. Li, *ACS Appl. Mater. Interfaces* **2017,** *9*, 27414.
[10] K. Lei, F. Li, C. Mu, J. Wang, Q. Zhao, C. Chen and J. Chen, *Energy Environ. Sci.* **2017,** *10*, 552.
[11] Q. Deng, J. Pei, C. Fan, J. Ma, B. Cao, C. Li, Y. Jin, L. Wang and J. Li, *Nano Energy* **2017,** *33*, 350.
[12] Y. Zhu, P. Chen, Y. Zhou, W. Nie and Y. Xu, *Electrochim. Acta* **2019,** *318*, 262.
[13] Y. Liang, C. Luo, F. Wang, S. Hou, S.-C. Liou, T. Qing, Q. Li, J. Zheng, C. Cui and C. Wang, *Adv. Energy Mater.* **2019,** *9*, 1802986.

[14] A. Slesarenko, I. K. Yakuschenko, V. Ramezankhani, V. Sivasankaran, O. Romanyuk, A. V. Mumyatov, I. Zhidkov, S. Tsarev, E. Z. Kurmaev, A. F. Shestakov, O. V. Yarmolenko, K. J. Stevenson and P. A. Troshin, *J. Power Sources* **2019,** *435*, 226724.
[15] M. Zhou, M. Liu, J. Wang, T. Gu, B. Huang, W. Wang, K. Wang, S. Cheng and K. Jiang, *Chem. Commun.* **2019,** *55*, 6054.
[16] Y. Hu, H. Ding, Y. Bai, Z. Liu, S. Chen, Y. Wu, X. Yu, L. Fan and B. Lu, *ACS Appl. Mater. Interfaces* **2019,** *11*, 42078.
[17] Z. Jian, Y. Liang, I. A. Rodríguez-Pérez, Y. Yao and X. Ji, *Electrochem. Commun.* **2016,** *71*, 5.
[18] M. Tang, Y. Wu, Y. Chen, C. Jiang, S. Zhu, S. Zhuo and C. Wang, *J. Mater. Chem. A* **2019,** *7*, 486.
[19] Z. Tong, S. Tian, H. Wang, D. Shen, R. Yang and C. S. Lee, *Adv. Funct. Mater.* **2020,** *30*, 1907656.
[20] F. A. Obrezkov, V. Ramezankhani, I. Zhidkov, V. F. Traven, E. Z. Kurmaev, K. J. Stevenson and P. A. Troshin, *J. Phys. Chem. Lett.* **2019,** *10*, 5440.
[21] F. A. Obrezkov, A. F. Shestakov, V. F. Traven, K. J. Stevenson and P. A. Troshin, *J. Mater. Chem. A* **2019,** *7*, 11430.
[22] R. R. Kapaev, I. S. Zhidkov, E. Z. Kurmaev, K. J. Stevenson and P. A. Troshin, *J. Mater. Chem. A* **2019,** *7*, 22596.
[23] Y. An, H. Fei, Z. Zhang, L. Ci, S. Xiong and J. Feng, *Chem. Commun.* **2017,** *53*, 8360.
[24] X. Xiao, L. Zou, H. Pang and Q. Xu, *Chem. Soc. Rev.* **2020,** *49*, 301.
[25] C. Li, K. Wang, J. Li and Q. Zhang, *Nanoscale* **2020,** *12*, 7870.
[26] Q. Deng, S. Feng, P. Hui, H. Chen, C. Tian, R. Yang and Y. Xu, *J. Alloys Compd.* **2020,** *830*, 154714.
[27] S. Su, Q. Liu, J. Wang, L. Fan, R. Ma, S. Chen, X. Han and B. Lu, *ACS Appl. Mater. Interfaces* **2019,** *11*, 22474.
[28] S.-Y. Li, W.-H. Li, X.-L. Wu, Y. Tian, J. Yue and G. Zhu, *Chem. Sci.* **2019,** *10*, 7695.
[29] X. Chen, H. Zhang, C. Ci, W. Sun and Y. Wang, *ACS Nano* **2019,** *13*, 3600.
[30] C. Zhang, Y. Qiao, P. Xiong, W. Ma, P. Bai, X. Wang, Q. Li, J. Zhao, Y. Xu, Y. Chen, J. H. Zeng, F. Wang, Y. Xu and J.-X. Jiang, *ACS Nano* **2019,** *13*, 745.